



## Open Archive Toulouse Archive Ouverte (OATAO)

OATAO is an open access repository that collects the work of Toulouse researchers and makes it freely available over the web where possible.

This is an author-deposited version published in: <http://oatao.univ-toulouse.fr/>  
Eprints ID: 16524

**To link to this article** : DOI: 10.1051/epjap/2013130080

URL : <http://dx.doi.org/10.1051/epjap/2013130080>

To cite this version: Bonnin, Xavier and Piquet, Hubert and Naudé, Nicolas and Chérif Bouzidi, Mohamed and Gherardi, Nicolas and Blaquièrre, Jean-Marc *Design of a current converter to maximize the power into homogeneous dielectric barrier discharge (DBD) devices.* (2013) European Physical Journal: Applied Physics, vol. 64 (n° 1). pp. 10901. ISSN 1286-0042

Any correspondence concerning this service should be sent to the repository administrator:  
[staff-oatao@listes-diff.inp-toulouse.fr](mailto:staff-oatao@listes-diff.inp-toulouse.fr)

# Design of a current converter to maximize the power into homogeneous dielectric barrier discharge (DBD) devices

Xavier Bonnin<sup>1,2,a</sup>, Hubert Piquet<sup>1,2</sup>, Nicolas Naudé<sup>1,2</sup>, Mohamed Chérif Bouzidi<sup>1,2</sup>, Nicolas Gherardi<sup>1,2</sup>, and Jean-Marc Blaquière<sup>1,2</sup>

<sup>1</sup> Université de Toulouse; INPT, UPS; LAPLACE (Laboratoire Plasma et Conversion d'Énergie); ENSEEIHT, 2 rue Charles Camichel, BP 7122, 31071 Toulouse cedex 7, France

<sup>2</sup> CNRS; LAPLACE, 31071 Toulouse, France

**Abstract.** This paper proposes a design approach of an electrical power supply intended to offer an especially well-suited supply mode, through the efficient control of the current injected into a DBD setup. The proposed topology is aimed at controlling the operating point of the electrical discharge, thereby allowing favoring the homogeneous regime, and maximizing the electrical power injected into the plasma. The power supply structure is designed on the basis of causality criteria and of an analytical analysis of the electrical waveforms, which are derived from an equivalent circuit model of the DBD. Design issues of this electrical generator are detailed and experimental analysis of its operation, together with actual performances are presented. A very good agreement is obtained by comparing simulation and experiments. Effective ability to control the power transfers by means of its two degrees of freedom (current magnitude and frequency) is highlighted.

## 1 Introduction

Dielectric barrier discharges (DBDs) are nowadays extensively used to achieve the generation of cold plasmas at atmospheric pressure [1, 2]; the dielectric barriers installed between the metallic electrodes of an AC discharge incorporate two main advantages: they maintain the plasma in the non-equilibrium regime and help distribute the microdischarges normally generated at high pressure over the entire electrode surface. Moreover it has been shown that in specific conditions, perfectly homogeneous discharges can be generated using DBDs [3]. These attributes are highly demanded in numerous processes, especially when relatively low temperatures are required, when the area to be affected by the effects of the plasma are large and when the costs associated with sophisticated vacuum units have to be avoided. Industrial applications of DBDs are spread out to various industrial domains, such as surface treatment [4–6], decontamination [7], semiconductor fabrication, lighting – especially UV rays generation [8] by means of DBD excimer lamps. Most of the time, efficiency criterion concerning the industrial process favors the injection of a maximized power. However, and in particular in the domain of surface treatments, the reliability of the process requires an accurate control of the elec-

trical power injected into the plasma, which in a second step defines the operating conditions of the discharge and thus the discharge regime (homogeneous or filamentary). Indeed, increasing the discharge power can result in microdischarges, which are strongly non-uniform and in some cases are not suitable for the deposition of smooth thin film without defects. As a contribution to the satisfaction of these needs, this paper proposes a design approach of an electrical power supply intended to offer an especially well-suited supply mode, through the efficient control of the current injected into the DBD setup. In homogeneous DBDs generated in nitrogen atmosphere, the discharge power is in fact limited due to the limitation of the slope of the voltage versus time and the maximal discharge current [9]. Thus, in the case of sinusoidal excitation, the amplitude and the frequency of the applied voltage that allows the homogeneous discharge regime are limited. A solution to increase the discharge power is to limit the current and to increase the discharge duration. This could be realized using a square-wave current inverter source [10].

Hence, in Section 2, the authors establish the merits of such current source generators [11]: on the basis of a classical electrical model of the DBD [12], analytical calculations are carried out and are used to compare a classical sinus voltage generator and a square shaped current source (the solution which is detailed in this paper); Section 3 is dedicated to the design of such a square shaped current

<sup>a</sup> e-mail: xavier.bonnin@laplace.univ-tlse.fr

source: an innovative topology is proposed and the dimensioning of its components is achieved. A special attention is paid to the step up transformer and the effects of its parasitic elements (leakage inductance, windings capacitances) are analyzed in details. Experiments carried on a prototype designed according to the previously defined relationships are finally proposed: they validate the expected performances detailed in Section 2 and the analysis concerning the transformers parasitic elements.

## 2 Supplying a DBD device with a current controlled power supply

In this section, we show that controlling the injected current allows to increase the injected power in a DBD device.

### 2.1 The electrical behavior of a DBD device

The particularity of a *Townsend* regime is that the voltage is almost constant, equal to  $\pm V_{th}$ , where  $V_{th}$  is the threshold voltage, whatever the current when the discharge is established (Fig. 1) [13]. The gas volume is delimited by two parallels electrodes covered by dielectrics, thus capacitive effects should be considered. These statements lead to the electrical model of the discharge presented Figure 2 [12].  $C_{gas}$  and  $C_{diel}$  are the equivalent capacitors of the gas and the solid dielectric, respectively [9, 10]. Their values are calculated assuming that the discharge section is equal to the entire electrode area.  $i_{dbd} - i_{gas}$  is the displacement current which does not produce any power. The threshold voltage represents the static behavior of the gas in the *Townsend* zone, presented in Figure 1. The current passing through this device is called the discharge current  $i_{gas}(t)$  which is responsible for power dissipation.  $C_{diel}$  represents the serial capacitance of the latter. Due to the presence of dielectric barrier,  $i_{dbd}$  has to be such as  $\langle i_{dbd} \rangle_T = 0$ , where  $\langle \cdot \rangle_T$  designates the average value calculated over a time interval of length  $T$ , being  $T$  the operating period.

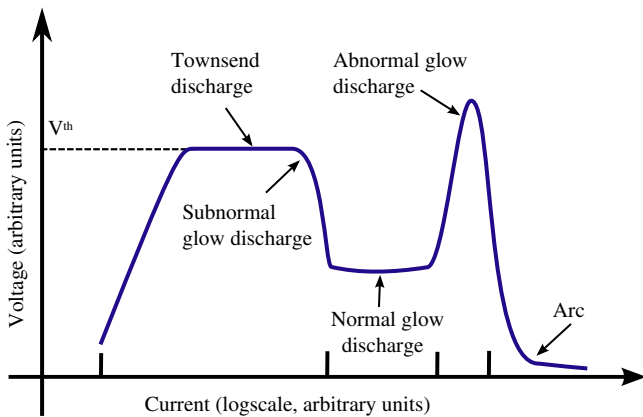


**Fig. 1.** Voltage-current characteristics of electrical discharge in gas at low pressure, with two planar electrodes.

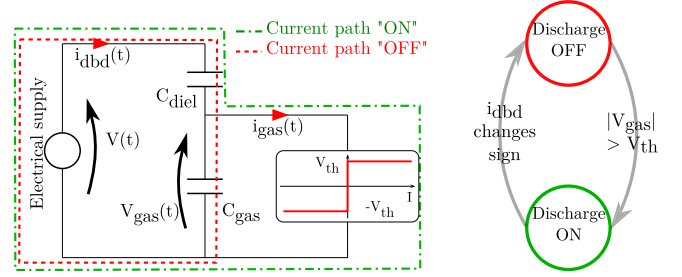


**Fig. 2.** Simple electrical behavioral model of a DBD device.

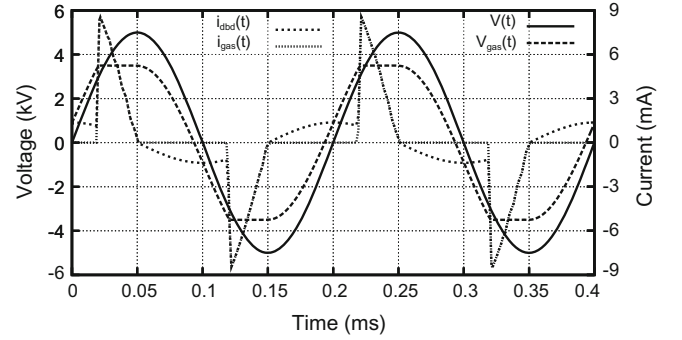


**Fig. 3.** Shape of  $V(t)$ ,  $V_{gas}(t)$ ,  $i_{dbd}(t)$  and  $i_{gas}(t)$  with a 5 kV/5 kHz sinusoidal voltage source.  $C_{gas} = 10$  pF,  $C_{diel} = 70$  pF and  $V_{th} = 3500$  V.

### 2.2 Effective control of the operating point in the DBD device

#### 2.2.1 With an AC voltage power supply

Considering the previously described circuit in Figure 2 we can see that the discharge current in the gas is given by

$$\begin{cases} i_{gas}(t) = C_{diel} \frac{dV}{dt} & \text{discharge ON} \\ i_{gas}(t) = 0 & \text{discharge OFF} \end{cases}, \quad (1)$$

and the gas voltage by

$$\begin{cases} V_{gas}(t) = V_{th} & \text{discharge ON} \\ V_{gas}(t) = \frac{C_{diel}}{C_{diel} + C_{gas}} V(t) & \text{discharge OFF} \end{cases}, \quad (2)$$

where  $V(t)$  is the voltage across the DBD device. Numerical simulation leads to the waveforms plotted on Figure 3. Assuming that  $V(t) = \hat{V} \cos(2\pi ft)$  and assuming that the gas changes from OFF state to ON state when the gas voltage reaches  $\pm V_{th}$ , and changes from ON state to OFF state when the discharge current vanishes (so, when the voltage source reaches an extremum) we find

$$P = 4fC_{diel}V_{th}\hat{V} \left( 1 - \left( 1 + \frac{C_{gas}}{C_{diel}} \right) \frac{V_{th}}{\hat{V}} \right), \quad (3)$$

where  $P$  is the mean injected power transferred to the DBD device. It is shown in (3) that the injected power

depends on both the frequency and the amplitude of the applied voltage which is consistent with experimental measurements. We note that a necessary condition to create power is that the amplitude of the applied voltage is greater than  $(1 + C_{\text{gas}}/C_{\text{diel}})V_{\text{th}}$  to allow the discharge ignition. Moreover, we note that the DBD device has a “instantaneous voltage source” behavior since it is a capacitive load. It means that the current in such a load can not be precisely controlled if supplied by a voltage source because it depends on the derivatives of the voltage applied (and so on its fast variations). Causality rules lead us to control the current injected in the load, letting the voltage being imposed by the DBD device behavior.

### 2.2.2 With an AC rectangular current power supply

**Waveforms and power transferred.** Whatever the current shape, we find that

$$\begin{cases} i_{\text{gas}}(t) = i_{\text{dbd}}(t), \\ V_{\text{gas}}(t) = \pm V_{\text{th}}, \end{cases} \quad (4)$$

when the discharge is “ON” and

$$\begin{cases} i_{\text{gas}}(t) = 0, \\ V_{\text{gas}}(t) = V_{\text{gas}}(t_0) + \frac{1}{C_{\text{gas}}} \int_{t_0}^t i_{\text{dbd}}(\tau) d\tau, \end{cases} \quad (5)$$

when the discharge is “OFF”,  $i_{\text{dbd}}(t)$  is the current flowing through the DBD device. For latter, we assume that the electrical supply presented in Figure 2 is a squarewave current source which frequency is  $f$ . Therefore we have  $i_{\text{dbd}}(t) = \pm I_{\text{DC}}$ . The theoretical waveforms of  $V_{\text{gas}}(t)$  and  $i_{\text{gas}}(t)$  are plotted Figure 4. When the current changes

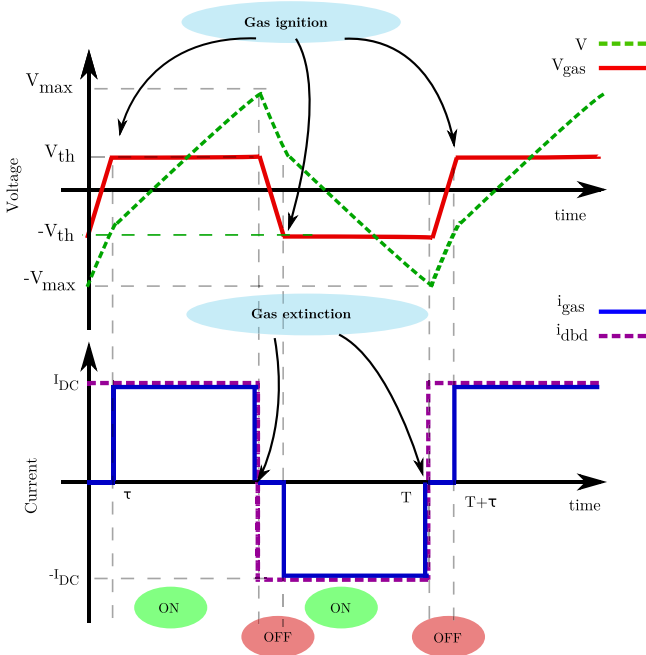


**Fig. 4.** Shape of  $V(t)$ ,  $V_{\text{gas}}(t)$ ,  $i_{\text{dbd}}(t)$  and  $i_{\text{gas}}(t)$ .

from  $-I_{\text{DC}}$  to  $+I_{\text{DC}}$  the operation can be decomposed in two sequences [10]:

- When the discharge is in the “OFF” state, the gas voltage is growing up from  $-V_{\text{th}}$  to  $+V_{\text{th}}$  with a slope  $I_{\text{DC}}/C_{\text{gas}}$  according to (5). During this time interval, no usable power is transferred into the plasma process, so the conduction current  $i_{\text{gas}}$  is zero. The duration  $\tau$  of this sequence is given by

$$\tau = \frac{2V_{\text{th}}C_{\text{gas}}}{I_{\text{DC}}}. \quad (6)$$

During this time interval, the transferred energy  $W$  is stored into  $C_{\text{gas}}$ . The latter takes the same value:

$$W = 1/2C_{\text{gas}}V_{\text{th}}^2, \quad (7)$$

at the beginning and at the end of  $\tau$  time interval, and is null when  $V_{\text{gas}}$  has a zero value.

- When the gas voltage reaches  $V_{\text{th}}$ , the discharges turns in the “ON” state and the current through the DBD device transfers power into the process; the displacement current is close to 0 (under the assumption that the gas voltage remains constant during the time interval during which the discharge is “ON”, then the displacement current is null). So, we have

$$V_{\text{gas}} = V_{\text{th}} \quad \text{and} \quad i_{C_{\text{gas}}} = 0.$$

The operating sequences are the same when the current  $i_{\text{dbd}}$  changes from  $+I_{\text{DC}}$  to  $-I_{\text{DC}}$  ... Therefore, the mean power transferred into the plasma process is given by

$$\begin{aligned} P &= 2f \int_{\frac{2V_{\text{th}}C_{\text{gas}}}{I_{\text{DC}}}}^{\frac{1}{2f}} I_{\text{DC}}V_{\text{th}} d\tau, \\ &= V_{\text{th}}I_{\text{DC}} \left( 1 - \frac{4V_{\text{th}}C_{\text{gas}}f}{I_{\text{DC}}} \right), \\ &= V_{\text{th}}I_{\text{DC}} (1 - 2\tau f), \\ &= V_{\text{th}}I_{\text{DC}} (1 - x), \end{aligned} \quad (8)$$

where  $f$  is the operating frequency, and  $\tau$  is given by (6). In order to simplify the notations the normalized variables  $r = C_{\text{gas}}/C_{\text{diel}}$  and  $x = 4V_{\text{th}}C_{\text{gas}}f/I_{\text{DC}} = 2\tau f$  has been introduced.

$2\tau f$  shows the normalized time to invert the polarity of the  $V_{\text{gas}}$  voltage and to change its value from  $-V_{\text{th}}$  to  $V_{\text{th}}$  under the current  $I_{\text{DC}}$  by one half-period. Considering the following usual orders of magnitude  $x$  is negligible compared to one if

- the operating frequency is in the range of several kilohertz,
- the discharge current density is higher than  $1 \text{ mA/cm}^2$ , which is a typical operating condition in nitrogen dielectric barriers controlled discharge,
- the gas gap is about few millimeters.

It proves that the injected power can be accurately adjusted with a current controlled power supply since, according to (8) and the previous assumptions,  $P \approx V_{\text{th}}I_{\text{DC}}$ .

**Maximum voltage.** One important quantity for designing such a current source with actual power electronics components is the operating voltage. This value can be calculated by integrating the current flowing through  $C_{\text{diel}}$  and the gas, considering that the mean value of  $C_{\text{diel}}$  voltage is zero. We find

$$V_{\text{max}} = \left(1 + \frac{r}{x}\right) V_{\text{th}}. \quad (9)$$

Typical value can be calculated considering that  $r$  is varying from 0.1 to 1 and  $x$  is about 0.01. We can see that the voltage can easily exceed several tens of kilovolts. Thereby, in order to accommodate with current power electronics components features, a high voltage transformer should be included in the design of this power converter. Insertion of a transformer leads to add its parasitic elements in the designing process. The quantities previously calculated (power, maximum voltage) should be a bit different from these given in (8) and (9). The way parasitic elements affect the waveforms is studied in Section 3.4.

### 3 Design of a rectangular current source

In this section we study the implementation of an AC rectangular current controlled power supply. We first develop considerations concerning the architecture and the design of such a generator. In a second step, we focus on the parasitic elements of the high voltage transformer and their effects on the waveforms and the performances. Demonstrations of the following equations can be found in [14]. Important elements from the specification for the design are remembered here:

- The designed generator is intended to be used for the research of the best suited supplying conditions, in order to maximize the electrical power injected into the plasma, while favoring the most homogeneous behavior of the plasma. In this scope a 5–15 kHz range has been selected for the frequency since it has proved to provide homogeneous discharges in nitrogen at atmospheric pressure with an AC voltage source supply.
- The maximal current density in the DBD device is about few mA/cm<sup>2</sup>. For experimental validations, a maximal current of 10 mA/cm<sup>2</sup> is chosen and a 9 cm<sup>2</sup> sample could be used: so we have to generate a current about 90 mA [3].
- The voltage we have to deal with is about tens of kilovolts since the gas threshold voltage is about 3500 volts (9) [13].

#### 3.1 Some design considerations

The main matter is to design a low-current square waveform power supply sustaining high voltage. A cascaded topology has been chosen; it includes two power converters (Fig. 5).

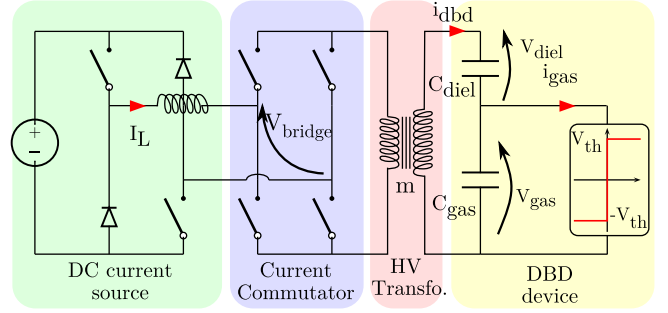


**Fig. 5.** A two-stages cascaded power converter to generate square waveform current.

- The first one is a tunable regulated DC current source.
- The second one allows to transform the DC current into an alternative square waveform current.

Although the high voltage transformer design is a very important aspect because of its parasitic elements, as developed in Section 3.4, its design is not treated in this paper.

Care must be taken when sizing the first stage component since the current ripple have to be quite low in order to generate a well suited current waveform. A four switches bridge is needed to produce the square shape current. The input voltage of the latter ( $V_{\text{bridge}}$  on Fig. 5) exhibits a sawtooth bidirectional waveform (Fig. 6b). So the DC current is controlled by means of a two quadrants chopper.

The switching frequency of the commutator depends on the plasma process specifications and should be tunable. It has been chosen to carry experimental investigations in the 5–15 kHz range. It does not need feedback-control since the commutator must only ensure that its duty cycle is 50% (that can be performed in an open-loop control with a well-designed modulator). Nevertheless, a DC component would bias the transformer's core and make it going on saturation if the duty cycle is not well controlled, drastically reducing the coupling between the primary and the secondary winding.

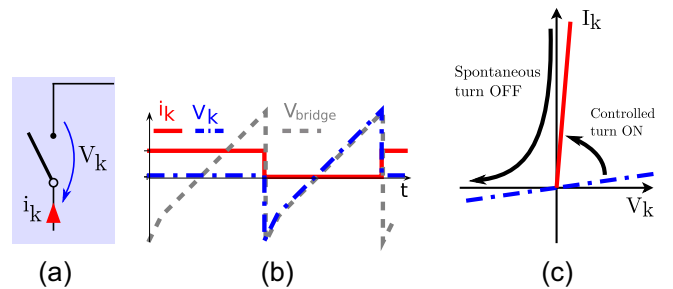


**Fig. 6.** Theoretical waveforms and commutator's switches characteristics.  $V_{\text{bridge}}$  (gray),  $I_K$  (red),  $V_k$  (blue). Figure (a) stands for the upper left commutator switch.

### 3.2 The commutator: synthesis of semiconductor switches

Theoretical waveforms concerning a commutator's switch Figure 6a are presented in Figure 6b. According to these waveforms, the upper-left switch static and dynamic characteristics are defined on Figure 6c. The same study carried out on the other commutator switches shows that they behave the same way.

Static characteristics are such that the switch should sustain positive and negative voltage, and conduct only positive current that confirms the use of 3-segments power switches (Fig. 6c). Analysis of the switchings show that it is

- turned on under a positive voltage conducting a positive current meaning a controlled turn on,
- turned off because of a zero crossing of its current (soft switching).

We recognize the behavior of a thyristor-like switch. Power synthesized thyristors such as presented in [15] should be used, because of the high switching frequency since current thyristor technology is not suitable for more than a few kHz.

### 3.3 The current source

The first stage of the power converter is made of a full-bridge topology. We can notice that basic designing rules would have led to work with a half-bridge topology (say a classical Buck step down chopper). Indeed, the current flowing through the switches is positive and the voltage that switches have to deal with is positive too. The matter is that even if the mean voltage drop seen after the inductance is positive ( $\langle V_{\text{bridge}} \rangle > 0$ ), it varies between negative and positive bounds (Fig. 6b). When it is negative, there is no switch configuration that would allow to decrease  $I_L$  value. Therefore, this leads to a temporary loss of the current value control during the time  $V_{\text{bridge}}$  is negative. Moreover, considering that the mean value of this voltage should be quite low compared to input voltage one, the duty cycle should be often close to zero which leads to technical problems because the ON time could be of the same order of magnitude as typical MOSFET switching time. Furthermore, another advantage of choosing a full-bridge topology is that it leads to work with a duty-cycle varying around a value slightly higher than 0.5. The features of this stage is to ensure the constancy of the inductance current value (called  $I_L$  on Fig. 5) although the output voltage  $V_{\text{bridge}}$  varies quickly. This specification can be honored by a fast control law as current-mode one. Current mode control leads underlying problem such as loss of stability when the ordered duty-cycle is above 50%. Ramp-compensation technique [16] has been used to overcome this problem.

**The first stage's power inductor sizing.** The value of  $L$  is chosen according to the well-known formula in the case

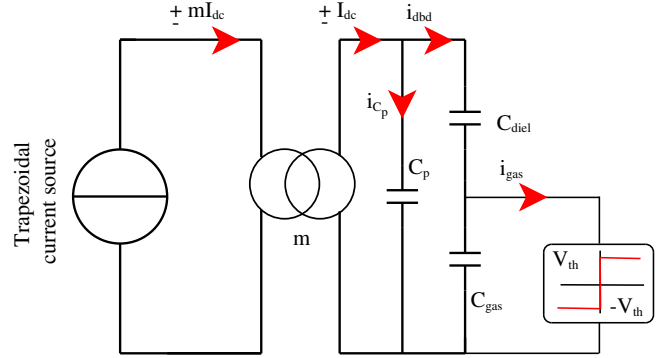


Fig. 7. Theoretical scheme taking into account the parasitic effects within the high voltage transformer.

of a two quadrants chopper:

$$\Delta I_L^{\max} = \frac{V_{in}}{2Lf}. \quad (10)$$

Thus, if  $V_{in} \approx 300$  V,  $f = 40$  kHz,  $mI_{DC} = 15$  A and if we want  $\Delta I_L$  to be lower than 5% of  $\langle I_L \rangle$ , we can choose  $L \approx 10$  mH. The core could be Fe-Si laminated based because the high frequency core losses are quite low because of the selected low value of  $\Delta I_L$ .

### 3.4 Influence of transformer's parasitic elements

Actual waveforms are quite different from that presented in Figure 4. Many parasitic effects due to the presence of the high voltage transformer affect the waveforms. A general scheme taking into account all these effects is presented Figure 7.  $L_\mu$  is the magnetizing inductance of the transformer,  $L_\ell$  is the leakage inductance and  $C_p$  serve at modeling the capacitive effects in the transformer. We study the three main effects: the capacitive effects in Section 3.4.1, the leakage inductance effect in Section 3.4.2 and the magnetizing inductance effect in Section 3.4.3.

#### 3.4.1 Parasitic capacitance

The current measured after the secondary winding is not rectangular because of the transformer capacitive parasitic effects. The consequence of capacitive effect is that a fraction of the injected primary current is derived through the dielectrics constituting the high-voltage transformer. Locating actual capacitive coupling is complex. However simplified analytical method convenient for modeling DBD device high-voltage transformers and design rules in order to minimize stray capacitance effects are proposed in [17]. However, we can consider that the leading effect can be represented as a capacitor connected between the transformer secondary winding terminals.

Considering the scheme Figure 7 and neglecting the other parasitic effects leads to write

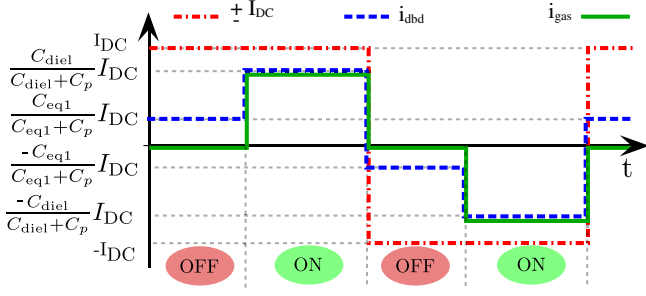


**Fig. 8.** Theoretical waveforms taking into account only the capacitive effects within the high voltage transformer.

$$\begin{cases} i_{\text{dbd}} = \pm \frac{C_{\text{diel}}}{C_{\text{diel}} + C_p} I_{\text{DC}} & \text{discharge ON} \\ i_{\text{dbd}} = \pm \frac{C_{\text{eq1}}}{C_{\text{eq1}} + C_p} I_{\text{DC}} & \text{discharge OFF} \end{cases}, \quad (11)$$

where  $C_{\text{eq1}} = C_{\text{diel}}C_{\text{gas}}/(C_{\text{diel}} + C_{\text{gas}})$  and  $I_{\text{DC}}$  is the theoretical rectangular waveform current amplitude we want to inject in the DBD. The general appearance of the waveforms are sketched Figure 8 from (11) taking into account only the capacitive effects. The main effect is that the time the discharge is ON is diminished compared to Figure 4.

Therefore the power transferred is diminished too. The ON time during a period is given by

$$t_{\text{ON}} = \left(1 - (1+r) \left(1 + r' + \frac{r'}{r}\right) x\right) \frac{1}{f}, \quad (12)$$

and the mean power transferred to the DBD device is given by

$$P = \frac{1}{1+r'} \left(1 - \left(1 + r' + \frac{r'}{r}\right) x\right) V_{\text{th}} I_{\text{DC}}, \quad (13)$$

where  $r = C_{\text{gas}}/C_{\text{diel}}$ ,  $r' = C_p/C_{\text{diel}}$ ,  $x = 4V_{\text{th}}C_{\text{gas}}f/I_{\text{DC}}$  and  $f$  is the switching frequency of the commutator. The experimental waveforms of Section 4.2 are obtained with a transformer which exhibits  $C_p \approx 100$  pF stray capacitance. The important influence  $C_p$  has on the performances of the system is highlighted in  $P(x)/(V_{\text{th}}I_{\text{DC}})$  plot Figure 9:  $C_p$  has to be minimized ( $r'$  minimized) by well designing the high-voltage transformer since the injected power  $P$  decreases as  $C_p$  increases for the same operating points at the primary side. Moreover,  $V_{\text{max}}$  is decreased by factor  $(1+r')$  giving

$$V_{\text{max}} = \frac{1+r/x}{1+r'} V_{\text{th}}. \quad (14)$$

It should be noticed that the way the transformer is grounded is an important aspect for the capacitive effects: the equivalent capacitance value strongly depends on that. In order to minimize its value, the ground connected to the magnetic core, should be also connected to the middle point of the secondary winding. This approach could not be always performed because it involves to work with two floating point, thus no electrode is actually connected to the ground.

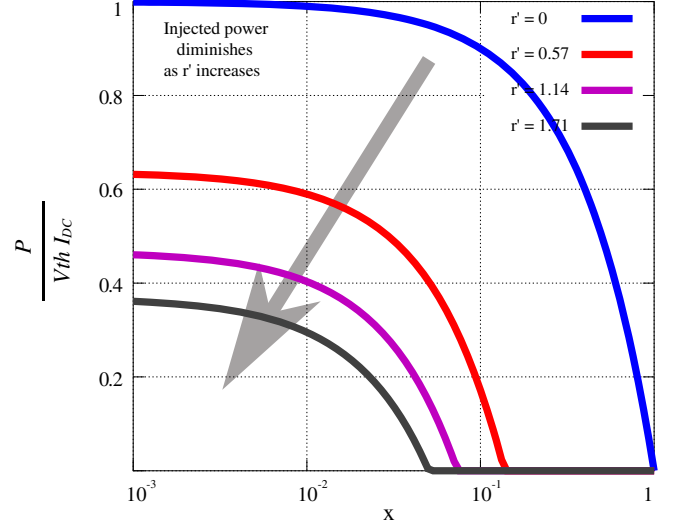


**Fig. 9.** Theoretical power plot versus  $x$  with  $r = 0.1$  showing the influence of  $C_p$  ( $r' = C_p/C_{\text{diel}}$ ).

### 3.4.2 Leakage inductance

In addition to the capacitive effects, the leakage inductance (considered at the primary winding) influences the waveforms and the commutator behavior. Since power switches are synthesized thyristors their spontaneous blocking state could not occur until the leakage inductance current has not reached  $\pm mI_{\text{DC}}$ , where  $m$  is the transformer ratio. Thus, reversing the current sign in the primary winding may take some time and steep transition can not be obtained and so the current waveform that can be generated at the primary winding has a trapezoidal shape instead of a square shape. When it is ordered that the primary current changes from  $+mI_{\text{DC}}$  to  $-mI_{\text{DC}}$  by switching ON the two blocked switches of the commutator, the voltage drop across the primary winding is about  $V_{\text{max}}/m$ ; see (9) for the  $V_{\text{max}}$  expression. Thus, the leakage inductance current has to change from  $+mI_{\text{DC}}$  to  $-mI_{\text{DC}}$  under a voltage  $V_{\text{max}}/m$  (we suppose that the voltage does not change significantly during the transition). Thus, the time this transition takes is then given by

$$t_t = 2m^2 \frac{1+r'}{1+r/x} \frac{L_\ell I_{\text{DC}}}{V_{\text{th}}}, \quad (15)$$

with the same notations as previously, where  $L_\ell$  is the leakage inductance value. To illustrate, a comparison is made in Figure 10. Theoretically, the transition time should be  $t_t = 4.12 \mu\text{s}$  using (15). Numerical simulations gives  $t_t \approx 4.55 \mu\text{s}$ . The difference between these values is due to the fact that the primary voltage is not really constant during the transition. We retain that (15) gives a good approximation of  $t_t$  anyway. When sizing the high voltage transformer, it must be ensured that the transition time can be neglected compared to the switching period. Therefore  $L_\ell$  should be such as

$$L_\ell \ll \frac{1+r/x}{1+r'} \frac{V_{\text{th}}}{2m^2 f I_{\text{DC}}}. \quad (16)$$

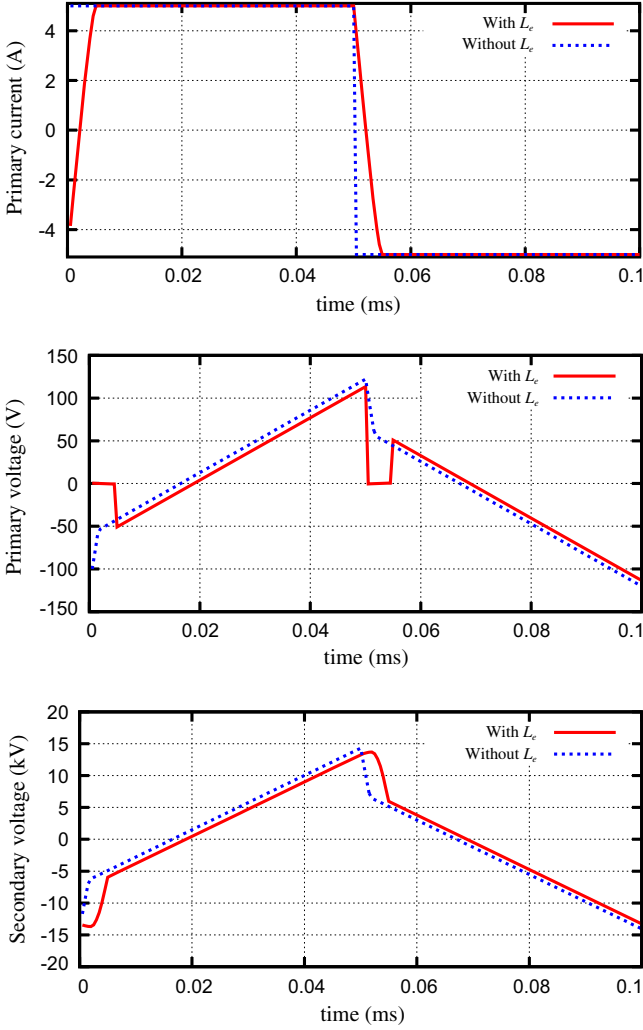


**Fig. 10.** Influence of  $L_\ell$ . PSIM simulation with  $f = 10$  kHz,  $I_L = 5$  A,  $C_p = 0$  pF,  $C_{\text{gas}} = 10$  pF,  $C_{\text{diel}} = 100$  pF,  $V_{\text{th}} = 3500$  V,  $m = 117$  and  $L_\ell = 50$   $\mu\text{H}$ .

Actually, a well suited high voltage transformer can satisfy the criterion (16) as long as the switching frequency is in a reasonable range (less than a few tens of kHz).

### 3.4.3 Magnetizing inductance

The role of the magnetizing inductance can be often neglected since its value can be well controlled when designing the high voltage transformer. Magnetizing inductance sinks a 180 degree dephased current compared to  $i_{\text{dbd}}$ , which slightly affects the current waveform (see experimental results in Sect. 4.2). Neglecting the effect of  $L_\ell$ , but taking into account the capacitive effects, the maximum value of the current absorbed by the magnetizing inductance is given by

$$I_\mu^{\text{max}} = \frac{V_{\text{th}}}{mL_\mu f} \left( \frac{A}{x} + Bx \right), \quad (17)$$

where  $L_\mu$  is the magnetizing inductance (considered at the primary winding side),  $I_\mu^{\text{max}}$  is the maximum current that

flows through  $L_\mu$  and the coefficients  $A$ ,  $B$  are given by

$$\begin{aligned} A &= \frac{r}{8(1+r')}, \\ B &= \frac{2rr' + 1 + 2r + 2r'}{8r(1+r')}. \end{aligned} \quad (18)$$

To ensure that the effect of  $L_\mu$  can be neglected, care must be taken to check that  $I_\mu^{\text{max}} \ll mI_{\text{DC}}$  when designing/choosing the high voltage transformer.

## 4 Implementation of the power converter and experimental results

The DBD device is made of two 9 cm<sup>2</sup> silver electrodes pasted on 0.635 mm thickness Al<sub>2</sub>O<sub>3</sub> dielectrics. The gas gap is about 1 mm. Parameters values are  $C_{\text{gas}} \approx 10$  pF,  $C_{\text{diel}} \approx 70$  pF and  $V_{\text{th}} \approx 3.9$  kV [9].

### 4.1 Implementation of the power converter

The power converter presented Figure 5 has been realized to conduct experimental campaigns in order to identify parameters which influence on the discharge behavior. The main characteristics are:

- It can provide a current  $I_L$  (Fig. 5) up to 15 A (in steady state) and work with an input voltage up to 400 V.
- The first stage switching frequency is fixed at 40 kHz, its inductance value is about 8 mH. The current  $I_L$  is tunable from 1 A to 15 A.
- The second stage switching frequency is tunable from 4 kHz to 17 kHz. The thyristor behavior is emulated by a MOSFET transistor in series with a diode, and an appropriate control law.
- The high voltage transformer we use exhibits a ratio of 155, a leakage inductance  $L_\ell$  of 18  $\mu\text{H}$ , a magnetizing inductance  $L_\mu$  of 16 mH, and an equivalent parasitic capacitance  $C_p$  of 100 pF.

### 4.2 Experimental results

Results at 5 kHz and 10 kHz are provided on Figures 11 and 12.

- The magnetizing inductance's effect is the change of the current shape at the secondary winding since a fraction of the injected current serves at magnetizing the transformer core.
- The leakage inductance make the current shape trapezoidal. During this transition time, the measured voltage drop across the primary winding of the power transformer vanishes since synthesized thyristors all are in the ON state (see Fig. 12).
- The parasitic capacitance effect is more important at high frequencies. It delays the gas breakdown absorbing a fraction of the injected current (this fraction of current is not the same depending on whether the discharge is alight or not). Therefore the measured current is lower than that it was expected.



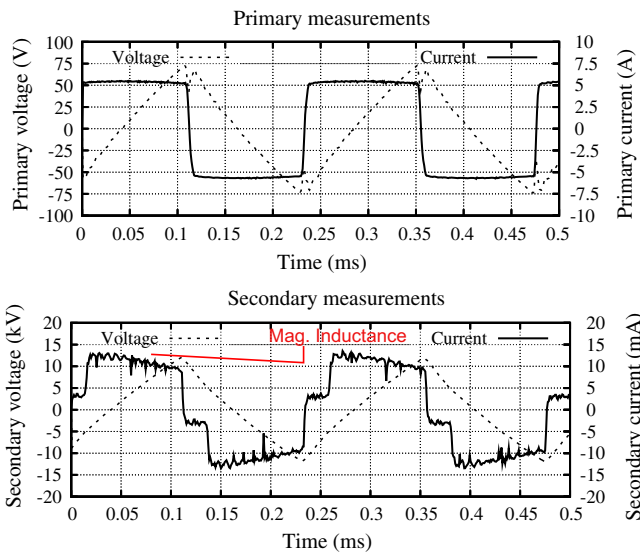


Fig. 11. Experimental results at 5 kHz (smoothed curves).

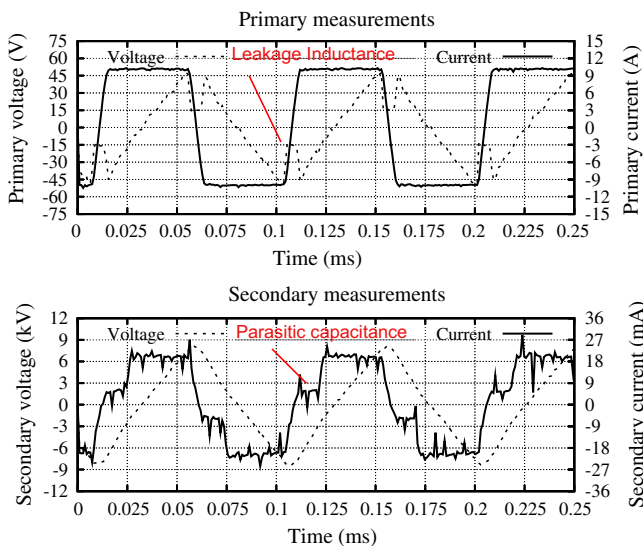


Fig. 12. Experimental results at 10 kHz (smoothed curves).

## 5 Conclusion

In this paper, the arguments for selecting a current controlled generator with a rectangular shape, in order to increase the amount of power injected into a DBD, and to maintain in the same time the electrical discharge in the homogeneous regime, have been evoked. The classical equivalent circuit of the DBD has shown to be of great interest in order to build the analytical relationships characterizing the electrical quantities of such a power supply. On this basis, an experimental setup has been designed and implemented. The effects of the parasitic elements of the step-up transformer inserted into the power transfer chain have been analyzed in details. The conclusions are clearly showing that the transformer is one of the key

components with respect to the effective control of the electrical power transferred into the gas, and that a great care has to be taken to control especially the parasitic capacitance as seen from the secondary winding, during the design of the latter. The proposed topology offers two degrees of freedom to control the operating conditions: the magnitude and the frequency of the rectangular current injected into the transformer. The output characteristics of the designed generator have been measured and are showing on the one hand a very good agreement with the expected theoretical ones, and on the other hand very promising performances, when compared with similar characteristics concerning a classical voltage source generator.

The authors are grateful to the French Midi-Pyrénées region for its support (PHPA project).

## References

1. U. Kogelschatz, *Plasma Chem. Plasma Proc.* **23**, 1 (2003)
2. F. Massines, A. Rabehi, P. Decomps, R.B. Gadri, P. Ségur, C. Mayoux, *J. Appl. Phys.* **83**, 2950 (1998)
3. F. Massines, N. Gherardi, N. Naudé, P. Ségur, *Eur. Phys. J. Appl. Phys.* **47**, 22805 (2009)
4. F. Massines, G. Gouda, N. Gherardi, M. Duran, E. Croquesel, *Plasma. Polym.* **6**, 35 (2001)
5. R. Seeböck, H. Esrom, M. Charbonnier, M. Romand, U. Kogelschatz, *Proceedings of the 7th International Conference on Plasma Surface Engineering, Surf. Coat. Technol.* **142–144**, 455 (2001)
6. C. Zhang, T. Shao, K. Long, Y. Yu, J. Wang, D. Zhang, P. Yan, Y. Zhou, *IEEE Trans. Plasma Sci.* **38**, 1517 (2010)
7. G. Vezzu, J.L. Lopez, A. Freilich, K.H. Becker, *IEEE Trans. Plasma Sci.* **37**, 890 (2009)
8. M. Lomaev, E. Sosnin, V. Tarasenko, D. Shits, V. Skakun, M. Erofeev, A. Lisenko, *Instrum. Exp. Tech.* **49**, 595 (2006)
9. N. Naudé, J.-P. Cambronne, N. Gherardi, F. Massines, *J. Phys. D: Appl. Phys.* **38**, 530 (2005)
10. S. Vongphouthone, H. Piquet, H. Foch, *Eur. Phys. J. Appl. Phys.* **15**, 123 (2001)
11. R. Díez, H. Piquet, M. Cousineau, S. Bhosle, *IEEE Trans. Ind. Electron.* **59**, 1912 (2012)
12. R. Díez, J.P. Salanne, H. Piquet, S. Bhosle, G. Zissis, *Eur. Phys. J. Appl. Phys.* **37**, 307 (2007)
13. Y.P. Raizer, *Gas Discharge Physics* (Springer Verlag, Berlin, 1991)
14. X. Bonnin, Master's thesis, INP Toulouse, ENSEEIHT, 2011
15. M. Cousineau, R. Díez, H. Piquet, O. Durrieu, *IEEE Trans. Ind. Electron.* **59**, 1920 (2012)
16. C. Basso and ON-Semiconductor, Application note AND8029/D Ramp Compensation for NCP1200, Technical report, ON Semiconductor, 2001
17. X. Bonnin, H. Piquet, D. Florez, R. Díez, Designing the high voltage transformer of power supplies for dbd: windings arrangement to reduce the parasitic capacitive effects, in *European conference on Power Electronics (EPE), 2013*